

# TRANSIENT ANALYSIS OF BLOOD FLOW IN FUSIFORM MODELS OF AORTIC ANEURYSMS

<sup>1</sup>R.VINOTH

**ABSTRACT--***The Computational Fluid Dynamic (CFD) models of idealized fusiform aortic aneurysms and aortic arch with saccular aneurysm were developed to estimate hemodynamic parameters. The transient flow was simulated in aortic aneurysm models with laminar flow condition. The wall of aortic aneurysm was treated as rigid. The hemodynamic parameters flow velocity, wall pressure and wall shear stress (WSS) were estimated from fusiform aneurysm models. These observed hemodynamic parameters shows that, the aneurysms with larger diameter may cause disturbed flow. The variation in peak wall pressure value in all models is minimum. The wall shear stress has attained high value at peak systole in all models. The flow velocity was estimated from saccular aneurysm models. The flow velocity result shows a recirculation of flow in the saccular aneurysm region. The calculated hemodynamic parameters may help to understand the insights of flow in aortic aneurysm models.*

**KEYWORDS:** *Aortic Aneurysm, Computational Fluid Dynamics, Transient Analysis, Wall Pressure, Wall Shear Stress, Flow Velocity.*

## I. INTRODUCTION

Aorta is the biggest blood vessel which transports blood from heart to other organs in a body. Aortic Aneurysm (AA) is bulging of particular segment of aorta. The most of the disease in cardiovascular system depends on the behavior of flow in that system [1, 2]. The analysis on flow in an aorta is crucial because the flow changes hemodynamic parameters which are acting on the wall. The interaction between the parameters and corresponding changes in wall is the major cause for formation of aortic aneurysm [3]. Hence, it is decided that the hemodynamic parameters plays an important role in aneurysm's rupture. The Computational Fluid Dynamics has been used for simulating flow in idealized models of aorta. The investigation of flow in arteries has been made easier by idealized artery models because the geometric parameters can be varied but other parameters can be held fixed in idealized model. The authors developed Fluid Structure Interaction (FSI) model of idealized Abdominal Aortic Aneurysm (AAA) to check the effect of spiral flow on hemodynamic parameters [4]. The investigation on aneurysm asymmetry in idealized computational fluid dynamics model of AAA done by the authors [5-7]. It is decided that the investigation on flow in aortic aneurysm is important to understand the insights of flow in aorta. The objective of this study is to develop Computational Fluid Dynamic models of an idealized fusiform aortic aneurysm using transient state conditions to understand the flow behavior. The blood flow around the aortic arch aneurysm is also simulated using CFD technique.

---

<sup>1</sup> Department of Electronics and Communication Engineering, Manipal Institute of Technology, Manipal Academy of Higher Education, Manipal, Karnataka, India

## II. METHODOLOGY

The geometry of idealized fusiform aortic aneurysm with  $D_{AA}$ , 30 mm and 60 mm was created by ANSYS Design Modeler (v14.5, ANSYS, Inc.). The methodology to create geometry of idealized aortic aneurysm and mesh refinement test for all the models were detailed in my previous publication [8]. The pulsatile velocity and pressure profiles were used at inlet and outlet of the model respectively for transient analysis. These profiles and other boundary conditions were shown in my previous publications [9, 10]. The geometry of aortic arch with saccular aneurysm was constructed using ANSYS Design Modeler (v14.5, ANSYS, Inc.) software as per geometrical data given in the literature [11] with slight modifications. The aortic arch was built as a 180° curved circular artery. A long inlet and outlet length was kept for aorta to get a stable and fully developed flow. The arch aneurysm was built as a spherical shape holding a smaller spherical bleb on top of aneurysm dome. In this model, Radius of the aortic arch is 3.4cm ; the diameter of the aorta is 1.3cm ; the radius of the aneurysm and the bleb are 1.1cm and 0.5cm respectively ; inlet and outlet length of the aorta 12 times of their diameter. The blood was considered as the isothermal, incompressible and laminar Newtonian flow. The cardiac cycle was taken as 1s. Time varying pulsatile boundary condition has been used to simulate the blood flow in a cardiac period and No-slip boundary conditions were used at all the vessel walls. The geometrical model was discretized into tetrahedral using ANSYS Workbench Meshing (v14.5, ANSYS, Inc.). The flow equations of transient conditions was solved by finite volume based software ANSYS CFX (v14.5, ANSYS, Inc.). In simulation, five cardiac cycles were used with 120 time steps of iteration in each cardiac cycle. All other profiles and boundary conditions were shown in my previous publications [9, 10].

## III. RESULTS AND DISCUSSION

The hemodynamic parameters are estimated at four different point of time and it will be displayed at that point of time. The velocity profiles of aortic aneurysm at four time instants in the cardiac cycle are shown in Figure 1. At  $t = 4.08s$  and  $t = 4.14s$ , the velocity has reduced in aneurysm region, but it increased at the entry portion of aneurysms. This happens because of sudden dilation of aorta. At  $t = 4.28s$ , the velocity is increased in the mid-section of aneurysm with  $D_{AA}=30$  mm and in the distal portion of aneurysm with  $D_{AA}=60$  mm. At  $t = 4.65s$ , the velocity has come down due to diastolic phase. The flow was streamline in both aneurysms at  $t = 4.08s$ . Two vortices occurred in the proximal portion of aneurysm with  $D_{AA}=60$  mm due to sudden expansion of area at  $t = 4.14s$ . At  $t = 4.28s$ , vortices are formed in both the aneurysm models and the intensity of vortices is high in aneurysm with  $D_{AA}=60$  mm due to higher diameter. The flow became asymmetric due to sudden expansion. This result is in good agreement with the result published in the literatures [12, 13]. The vortex flow allows extended contact of the small bits of protoplasm with the lumen surface and this vortices increases the platelets deposition in the lumen surface [14]. This deposition raises thrombus renewal and it can cause rupture of aneurysm. At  $t = 4.65s$ , the flow is decelerated in the aneurysm models. The flow velocity varies in the range between 0.000 m/s and 0.940 m/s. The maximum value of velocity of 0.940 m/s was obtained in the aneurysm model with  $D_{AA}=60$  mm at peak systole. The velocity has reached its peak value in the mid portion of flow in all

models. The extremely disturbed and vortex flow had obtained in the dilated portion of aneurysms, it had found from the clinical observations these are the spots where aortic dissection frequently happens. These observation shows that, the aneurysms with larger diameter may cause disturbed flow and it may cause acute damage to the aortic wall. Figure 2 presents wall pressure distribution of aortic aneurysms at four time instants in the cardiac cycle. The wall pressure of aortic aneurysm decreases in flow direction at  $t = 4.08s$ . In aortic aneurysm with  $D_{AA} = 30$  mm the wall pressure decreased from the inlet to the expansion region of aneurysm, increased along the aneurysm and again decreased from the contraction region of aneurysm to outlet at peak systole. At same time instant, the wall pressure value (12169.988 Pa) of aortic aneurysm with  $D_{AA} = 60$  mm is the highest value of all the models. At  $t = 4.28s$ , the wall pressure value is increased in the flow direction. The pressure value of all the models at this time instant is more than other pressure values at other three time instants. The wall pressure value at this time instant is the peak value because the pressure waveform which is fixed as boundary condition at the outlet of aorta has peak value at  $t = 4.31s$ . At mid-diastole, again the wall pressure declined in flow direction. In aortic aneurysm with  $D_{AA} = 60$  mm, the wall pressure has attained its peak value at the contraction point of aneurysm and this is the region where aneurysm ruptures [15]. The wall pressure result shows that, there is no much variation in peak value of all the models at corresponding time instants due to pulsatile flow. This result has proved that the consequence of aneurysm's shape and size on the pressure distribution was small. The authors [14, 16] found qualitative result of pressure distribution similar to the present work. Figure 3 shows wall shear stress distribution of aortic aneurysms at four time instants in the cardiac cycle. WSS is a stress component and it is tangential force applied on the vessel surface by flow. The WSS distribution along the aneurysm wall explains the mechanism of platelet deposition along the aneurysm sac. At  $t = 4.08s$  and  $4.14s$ , the wall shear stress is reduced in aneurysm due to sudden dilation of aorta but it increases at contraction point due to sudden contraction of aorta. The WSS value is maintained approximately 1.5 Pa in aneurysm with  $D_{AA} = 30$  mm at  $t = 4.08s$ . At  $t = 4.14s$ , WSS value is observed nearly zero in aneurysm region. The wall shear stress is distributed abnormally (high/low) in aneurysm region at other two time instants. The wall shear stress has attained high value at peak systole in all the models. The result expresses that, the shear stress value is high on aortic wall at peak flow and high/low shear can occur during deceleration phase. The abnormal WSS may cause aneurysm growth in the aneurysm region. The results of velocity streamline of saccular aneurysm were depicted at two time instant of cardiac cycle. The two instants are flow acceleration phase and flow deceleration phase. Figure 4 shows the velocity streamline in the saccular aneurysm. This picture shows both inward and outward flow regions of the aneurysm. At  $t = 4.08s$ , the fluid enters at left hand side of the aneurysm and leaves from right hand side of the aneurysm. The velocity varies in the range of 0.01225 m/s to 0.8844 m/s. The velocity is distributed uniformly in the aortic arch during the flow acceleration phase. This uniform distribution of flow velocity may not cause any damage to the aortic walls. At  $t = 4.28s$ , the fluid gets into the aneurysm at right hand side and gets out from the aneurysm at left hand side. This type of flow recirculation may damage the aortic walls at the entry point of flow. This is the region where aortic arch dissection happens. This change in flow vertex happens due to the pulsatile flow. The velocity varies in the range of 0.002349 m/s to 1.278 m/s. The flow is not uniformly distributed during the flow deceleration phase. The flow shows higher velocity at the upper regions of aortic arch and this higher velocity may cause damage to the aortic walls. This damage leads to aortic arch dissections. This type dissections may lead to death of patients.

#### IV. LIMITATIONS

Idealized models of aortic aneurysms as shown in Figure 5 were implemented in this study, but to estimate the right hemodynamic parameters from the simulation the realistic geometry conditions of aorta are to be considered. The elasticity property of aortic wall has to be considered for the simulations of flow in the aorta. Actually the blood is a non-Newtonian fluid, here it is assumed as Newtonian fluid. The blood has to be assumed as non-Newtonian fluid. In this study, calcifications and intraluminal thrombus (ILT) were not considered. The hemodynamic parameters estimated here only not sufficient to predict the aneurysm rupture and structural parameters like stress analysis also important to predict the aneurysm rupture. All the above important assumptions for flow study in the aortic models will be included in my future study of flow analysis in aorta models.

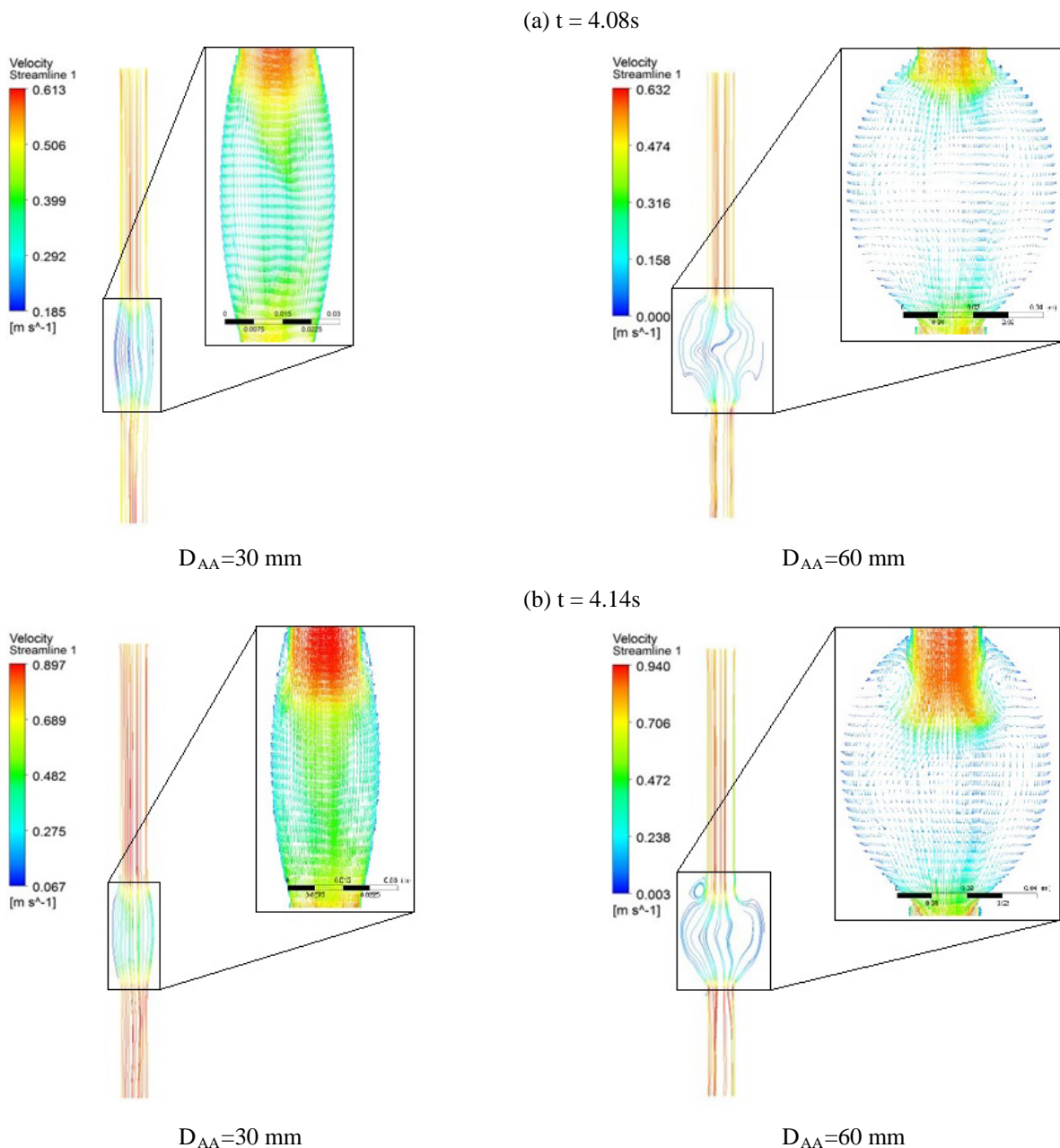
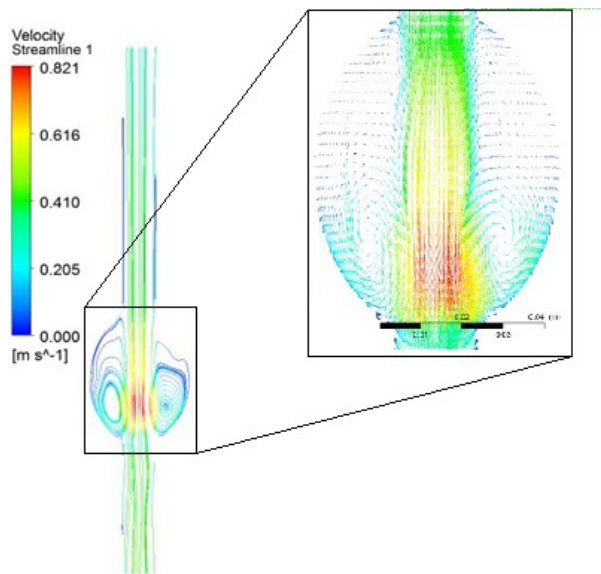
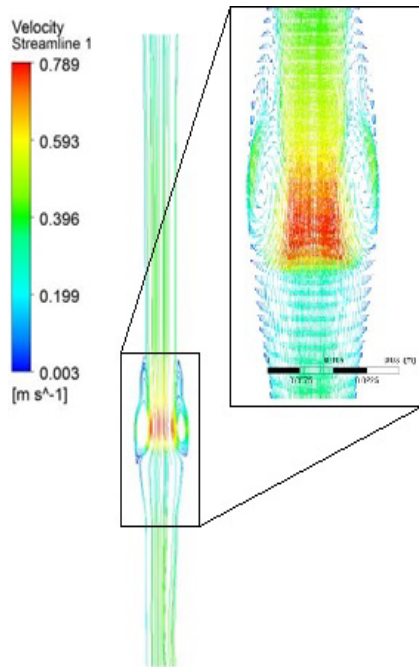


**Figure 1:** Flow streamlines of idealized aortic aneurysm with  $D_{AA}$ , 30 mm and 60 mm. The insert figures in the upper right corner of each panel show the velocity vector distribution in the aneurysm region.

**Figure 1: Continued**

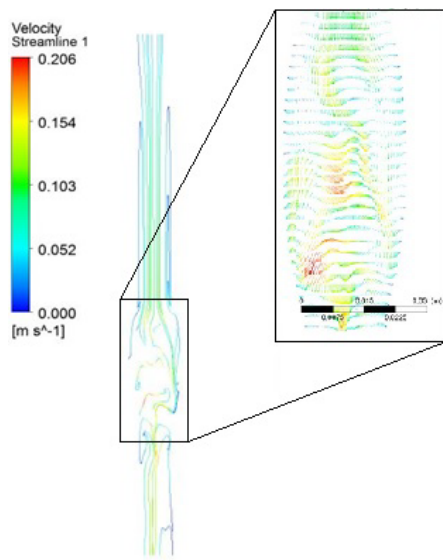
(c)  $t = 4.28$



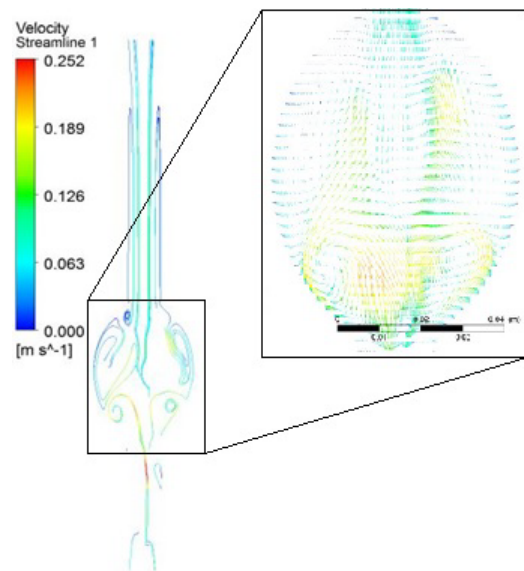
$D_{AA} = 30$  mm

$D_{AA} = 60$  mm

(d)  $t = 4.65$ s

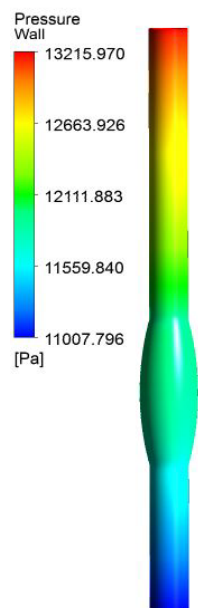


$D_{AA}=30$  mm

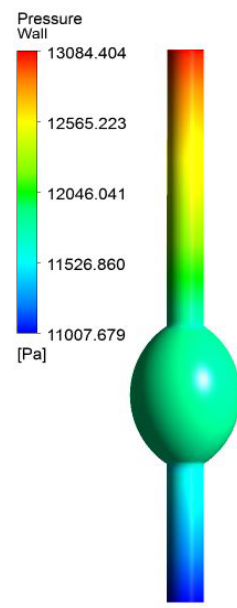


$D_{AA}=60$  mm

(a)  $t = 4.08$ s

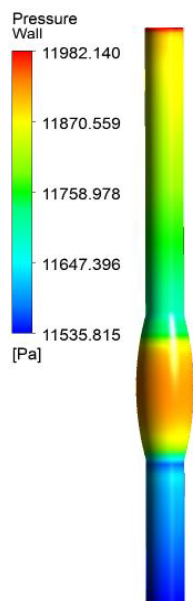


$D_{AA}=30$  mm

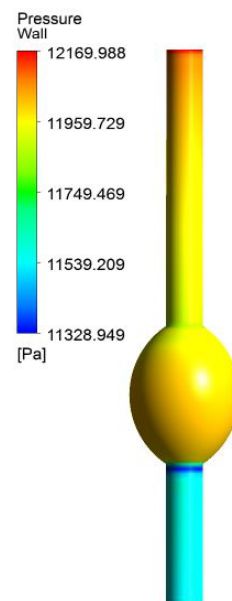


$D_{AA}=60$  mm

(b)  $t = 4.14$ s



$D_{AA}=30$  mm

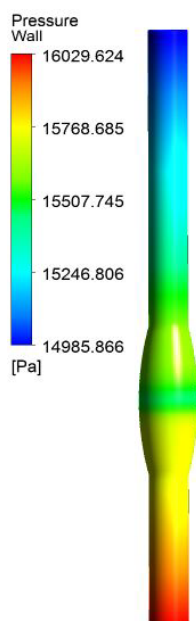


$D_{AA}=60$  mm

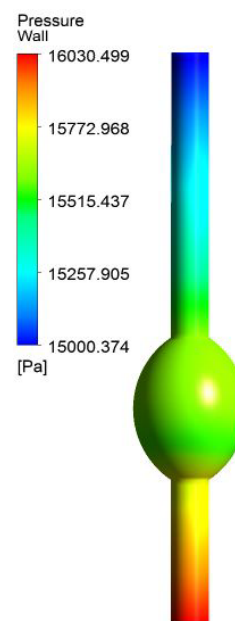
**Figure 2:** Wall pressure of idealized aortic aneurysm with  $D_{AA}$ , 30 mm and 60 mm

**Figure 2:** Continued

(c)  $t = 4.28$ s

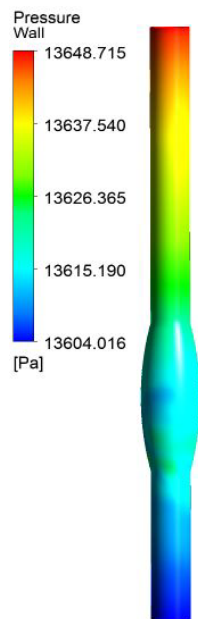


$D_{AA}=30$  mm

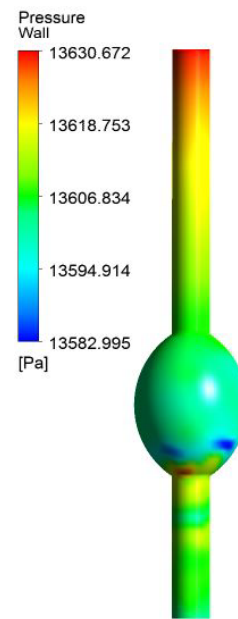


$D_{AA}=60$  mm

(d)  $t = 4.65$ s

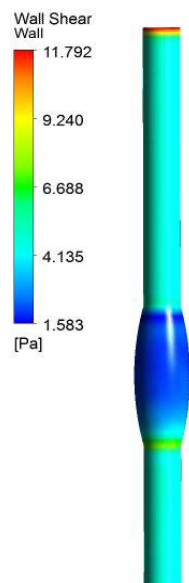


$D_{AA}=30$  mm

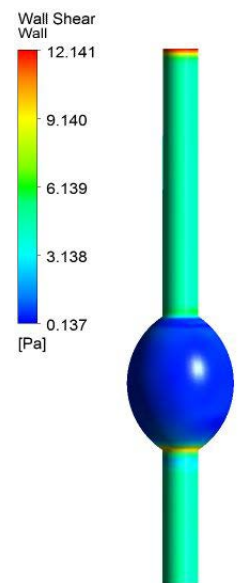


$D_{AA}=60$  mm

(a)  $t = 4.08s$



$D_{AA}=30$  mm



$D_{AA}=60$  mm

(b)  $t = 4.14s$

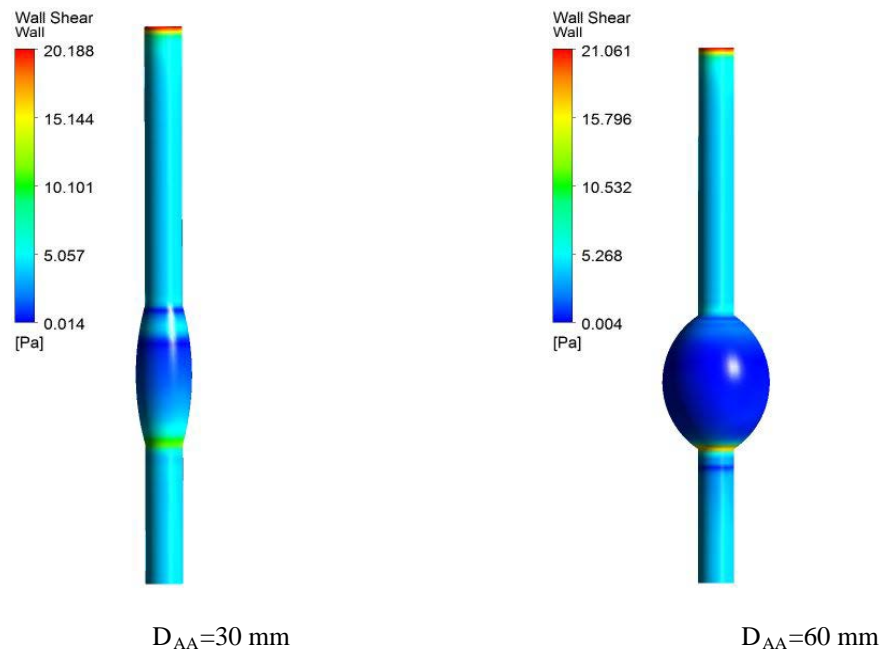
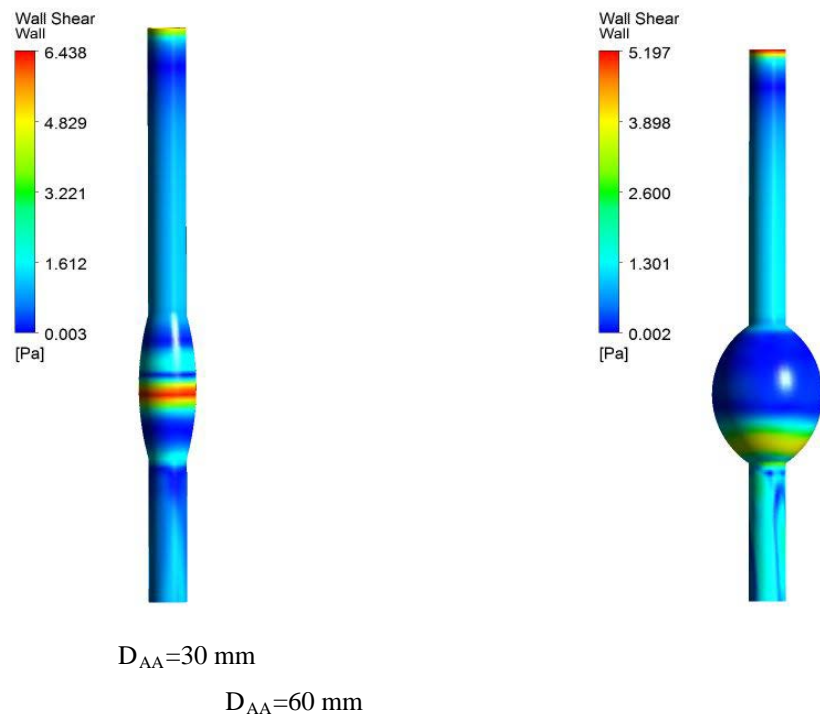


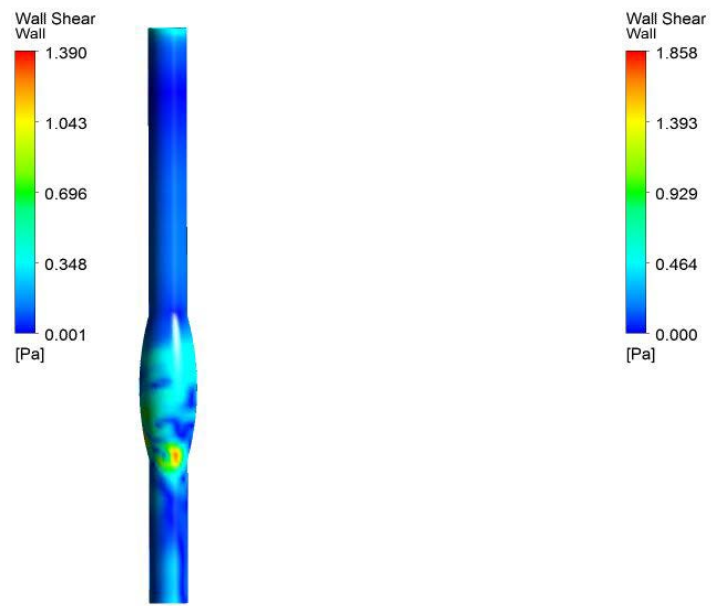
**Figure 3:** Wall shear stress of idealized aortic aneurysm with  $D_{AA}$ , 30 mm and 60 mm.

**Figure 3: Continued**

(c)  $t = 4.28$ s



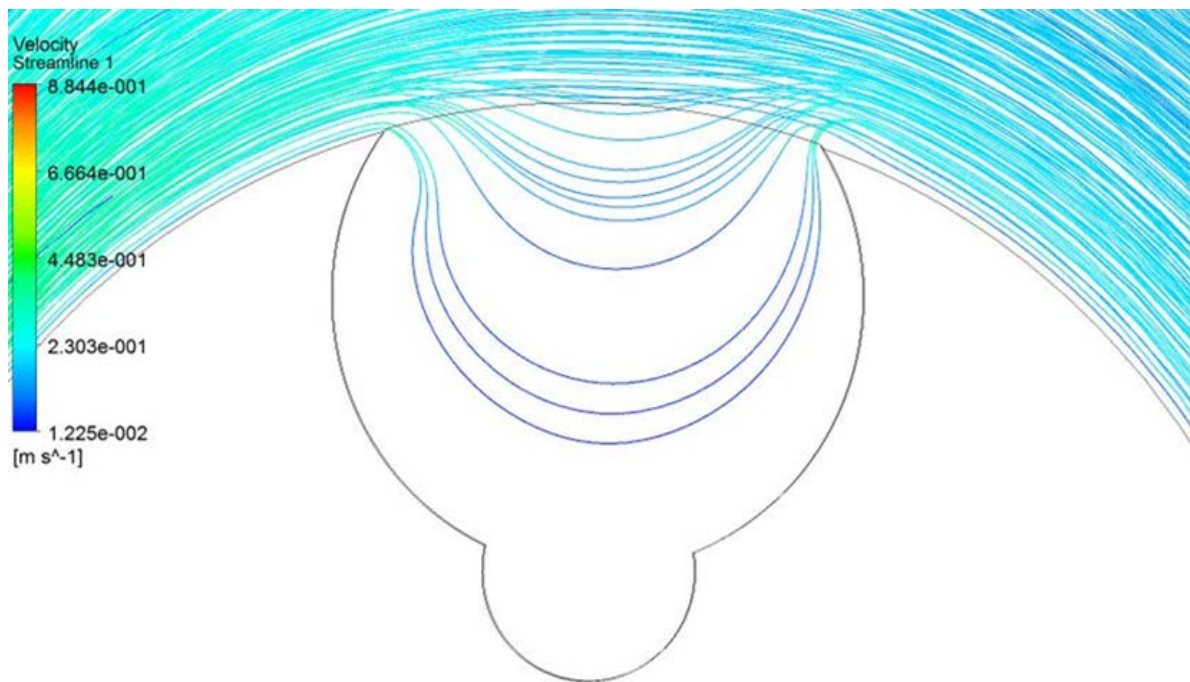
(d)  $t = 4.65$ s



$D_{AA}=30$  mm

$D_{AA}=60$  mm

(a)  $t = 4.08$ s



(b)  $t = 4.28$ s

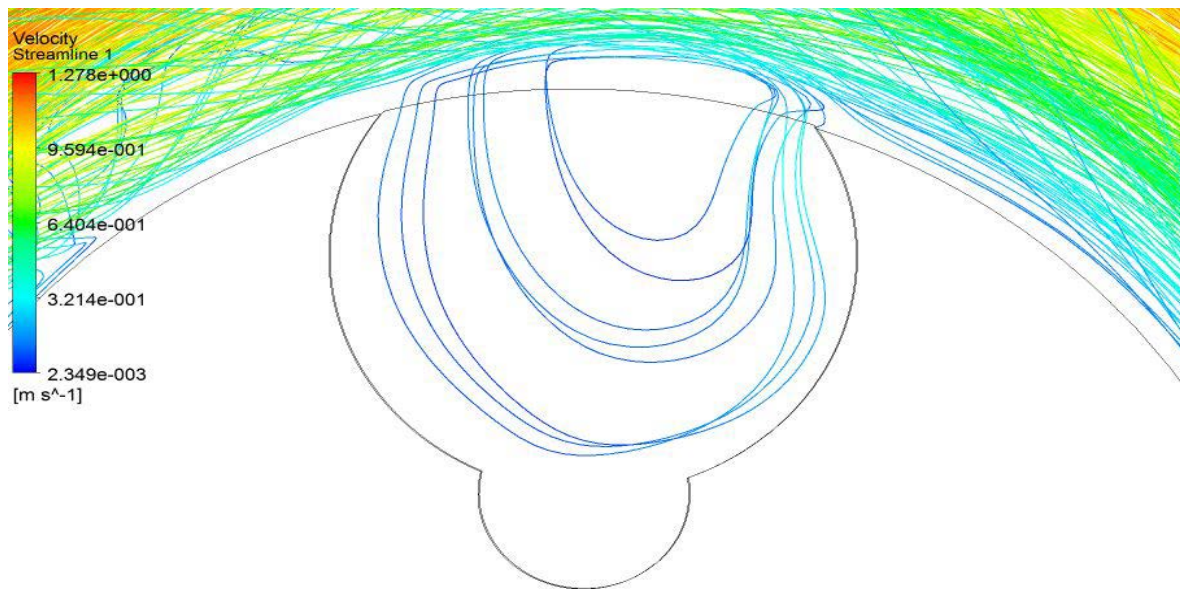


*Figure 4: Velocity streamline.*



$D_{AA}=30$  mm



$D_{AA}=60$  mm

*Figure 5: Idealized models.*

## V. CONCLUSION

The transient flow through aneurysmal aorta with different aneurysm diameters and aortic arch aneurysm under laminar flow condition has been simulated using CFD technique. The flow streamline, wall pressure and wall shear stress were presented at four time instants in the cardiac cycle. The flow streamlines had manifested that, the high flow velocity could happen in the aneurysm with larger size. The wall pressure result demonstrated that, there is a less variation in peak value of all the models at corresponding time instants due to pulsatile nature of flow. The WSS results depicted that, the high/low shear stress could occur in the aneurysm during deceleration phase of flow. The flow velocity streamline in arch aneurysm depicted that, the flow recirculation could occur in the saccular aneurysm region. These results may help the surgeons to understand the condition of the aortic aneurysm disease.

## REFERENCES

1. Moayeri, M.S and Zendehbudi, G. R, (2003). Effects of elastic property of the wall on flow characteristics through arterial stenosis. *Journal of Biomechanics*, 36, pp525-535.
2. Singh, S, (2011). Effects of shape of stenosis on arterial rheology under the influence of applied magnetic field. *International Journal of Biomedical Engineering and Technology*, 6(3), pp286–294.
3. Salsac, A.V, Sparks, S.R, Chomaz, J.M and Lasheras, J.C, (2006). Evolution of the wall shear stresses during the progressive enlargement of symmetric abdominal aortic aneurysms. *Journal of Fluid Mechanics*, 560, pp19-51.
4. AshkanJavadzadegan, BabakFakhim, MehrdadBehnia and MasudBehnia, (2014). Fluid-structure interaction investigation of spiral flow in a model of abdominal aortic aneurysm. *European Journal of Mechanics B/Fluids*, 46, pp109-117.
5. Finol, E.A, Keyhani, K and Amon, C.H, (2003). The effect of asymmetry in abdominal aortic aneurysms under physiologically realistic pulsatile flow conditions. *Journal of Biomechanical Engineering*, 125, pp207-217.
6. Salsac, A.V, Sparks, S.R and Lasheras, J.C, (2004). Haemodynamics changes occurring during the progressive enlargement of abdominal aortic aneurysms. *Annals of Vascular Surgery*, 18, pp14-21.
7. Singh, G. D. Design and Optimization of Crankshaft for Four Cylinder 4-Stroke Spark Ignition Engine using Transient Structural Analysis.
8. Venkatasubramaniam, A.K, Fagan, M.J, Mehta, T, Mylankal, K.J, Ray, B, Kuhan, G, Chetter, I.C and McCollum, P.T, (2004). A comparative study of aortic wall stress using finite element analysis for ruptured and non-ruptured abdominal aortic aneurysms. *European Journal of Vascular and Endovascular Surgery*, 28, pp168-176.
9. R.Vinoth, D.Kumar, RavirajAdhikari, DedeepiyaDevaprasad, DhamodharanKaliyamoorthy, (2015). Computational Investigation of Blood Flow in Fusiform Models of Aortic Aneurysms: A Steady State Analysis. *International Journal of Biomedical Engineering and Technology*, 19(1), pp70-91.
10. Ravishankar, P., Chakraborty, P., & Saravanan, A. Periodontal Disease–A Risk of Cardiovascular Disease.

11. Vinoth. R, Kumar. D, RavirajAdhikari, Vijay Shankar. CS, (2017). Non-Newtonian and Newtonian Blood Flow in Human Aorta: A Transient Analysis. *Biomedical Research*, 28(7), pp3194-3203.
12. Habeeb-Allah, A. M., & Alasad, J. Delirium Post Cardiac Surgery: Review on Epidemiology and Associated Risk Factors.
13. R.Vinoth, (2018). Transient Analysis of Blood Flow in Idealized Aorta. *International Journal of Mechanical Engineering and Technology*, 9(12), pp1090-1094.
14. Aike Qiao and Youjun Liu, Hemodynamics Simulation of Partly Stented Aortic Arch Aneurysm. First international conference on bioinformatics and biomedical engineering, 6-8 July 2007.
15. Jayaprakash, S., & Aralapuram, K. Clinical and Angiographic Profile of Patients with Symptomatic peripheral Arterial Disease.
16. Mullin.T, Shipton. S and Tavener. SJ, (2003). Flow in a symmetric channel with an expanded section. *Fluid Dynamic Research*, 33, pp 5-6.
17. Juan Lasheras, (2007). The Biomechanics of Arterial Aneurysms. *Annual Review of Fluid Mechanics*, 39, pp293-319
18. Vijay, P. M., & Prakash, A. M. A. R. (2014). Analysis of sloshing impact on overhead liquid storage structures. *International Journal of Research in Engineering & Technology*, 2(8).
19. Bluestein. D, Niu. L, Schoepfoerster. R.T and Dewanjee. M.K, (1996). Steady flow in an aneurysm model: correlation between fluid dynamics and blood platelet deposition. *ASME Journal of Biomechanical Engineering*, 118(3), pp.280-286.
20. Muraki, N. (1983). Ultrasonic Studies of the Abdominal Aorta with Special Reference to Hemodynamic Considerations on Thrombus Formation in the Abdominal Aortic Aneurysm. *Journal of Japanese College Angiology*, 23, pp401-413.
21. Miriyala, S., Ram, B. S., & Anjaneyulu, K. Fault Detection of Power Transformer by using Wavelet Transforms.
22. Taylor. T.W and Yamaguchi. T. (1994). Three Dimensional Simulation of Blood Flow in an Abdominal Aortic Aneurysm-Steady and Unsteady Flow Cases. *Journal of Biomechanical Engineering*, 116, pp.89-
23. Harikesh maurya, susheel kumar dubey, poonam bisht, monika semwal, sanjay gandhi (2016) an updates on the sepsis causing multiple organ dysfunctions. *Journal of Critical Reviews*, 3 (3), 31-40.
24. Caponigro, M., Jiang, X., Prakash, R., Vimal, R.L.P. Quantum Entanglement: Can we "See" the implicate order? *Philosophical Speculations* (2010) *NeuroQuantology*, 8 (3), pp. 378-389.
25. Mender, D. From quantum wetware to mental illness: A section editor's first interim progress report (2010) *NeuroQuantology*, 8 (2), pp. 115-119.